Bioorganic & Medicinal Chemistry Letters 27 (2017) 4714–4724

Contents lists available at ScienceDirect

Bioorganic & Medicinal Chemistry Letters

journal homepage: www.elsevier.com/locate/bmcl

Structure-activity relationship study of small molecule inhibitors of the DEPTOR-mTOR interaction

Jihye Lee [a,d,1,2], Yijiang Shi [b,c,d,1], Mario Vega [b,c], Yonghui Yang [b,c], Joseph Gera [b,c,d,e,1], Michael E. Jung [a,c,d,*,1], Alan Lichtenstein [b,c,d,e,*,1]

[a] Department of Chemistry and Biochemistry, University of California Los Angeles, Los Angeles, CA 90095, USA
[b] Department of Medicine, David Geffen School of Medicine, University of California Los Angeles, Los Angeles, CA 90095, USA
[c] Jonnson Comprehensive Cancer Center, University of California Los Angeles, Los Angeles, CA 90095, USA
[d] Molecular Biology Institute, University of California Los Angeles, Los Angeles, CA 90095, USA
[e] Department of Research and Development, Greater Los Angeles Veterans Affairs Healthcare System, Los Angeles, CA 91343, USA

ARTICLE INFO

Article history:
Received 18 May 2017
Revised 1 September 2017
Accepted 1 September 2017
Available online 6 September 2017

Keywords:
mTOR
DEPTOR
Multiple myeloma
Cytotoxicity
SAR study

ABSTRACT

DEPTOR is a 48 kDa protein that binds to mTOR and inhibits this kinase within mTORC1 and mTORC2 complexes. Over-expression of DEPTOR specifically occurs in the multiple myeloma (MM) tumor model and DEPTOR knockdown is cytotoxic to MM cells, suggesting it is a potential therapeutic target. Since mTORC1 paralysis protects MM cells against DEPTOR knockdown, it indicates that the protein–protein interaction between DEPTOR and mTOR is key to MM viability vs death. In a previous study, we used a yeast two-hybrid screen of a small inhibitor library to identify a compound that inhibited DEPTOR/mTOR binding in yeast. This therapeutic (compound B) also prevented DEPTOR/mTOR binding in MM cells and was selectively cytotoxic to MM cells. We now present a structure–activity relationship (SAR) study around this compound as a follow-up report of this previous work. This study has led to the discovery of five new leads – namely compounds 3g, 3k, 4d, 4e and 4g – all of which have anti-myeloma cytotoxic properties superior to compound B. Due to their targeting of DEPTOR, these compounds activate mTORC1 and selectively induce MM cell apoptosis and cell cycle arrest.

DEPTOR is a recently described protein that binds to mTOR and inhibits this kinase within mTORC1 and mTORC2 complexes.[1] As an inhibitor of mTOR, it is not surprising that DEPTOR's expression is quite low in most tumor types.[1] However, over-expression of DEPTOR occurs in the multiple myeloma (MM) tumor model with highest levels found in the specific genetic categories of MM that contain translocations between the IgH and MAF genes or copy number gains at chromosome 8q24[2], a region that contains the DEPTOR gene. DEPTOR knockdown in high DEPTOR-expressing MM cell lines induces growth arrest and apoptosis. The anti-MM effects of DEPTOR silencing and singular over-expression in MM suggest DEPTOR is a potential therapeutic target in this malignancy.

Since DEPTOR is an mTOR inhibitor, the proximal molecular effect of DEPTOR knockdown is activation of mTORC1 and mTORC2 activity. The finding that mTORC1 paralysis protects MM cells against DEPTOR knock-down[1,3] indicates that DEPTOR binding to mTOR with resulting mTORC1 inhibition contributes to MM viability and proliferation. To this end, in a previous study[4], we designed a yeast two-hybrid screen, interrogating a small inhibitor library for compounds that could inhibit DEPTOR/mTOR binding in yeast. We identified a hit compound (compound **B**) which also prevents mTOR/DEPTOR binding within MM cell lines, acutely activates mTORC1 and selectively induces MM cell apoptosis and cell cycle arrest.[4] Anti-MM cell cytotoxicity was directly correlated with the levels of DEPTOR expression in a panel of MM cell lines. This compound is also effective in vivo in a murine xenograft model of MM growth, is cytotoxic to primary MM cells, and is remarkably non-toxic to normal hematopoietic colony forming cells and without observable side effects when used in mice. In a surface plasmon resonance assay, our lead compound **B** bound to recombinant DEPTOR but not mTOR.

* Corresponding authors at: Department of Chemistry and Biochemistry, University of California Los Angeles, Los Angeles, CA 90095, USA (M.E. Jung). Jonnson Comprehensive Cancer Center, University of California Los Angeles, Los Angeles, CA 90095, USA (A. Lichtenstein).

E-mail addresses: jung@chem.ucla.edu (M.E. Jung), alan.lichtenstein@med.va.gov (A. Lichtenstein).

[1] These authors contributed equally.

[2] Current address: Neuroscience Research Institute, Gachon University, 24, Namdong-daero 774 beon-gil, Namdong-gu, Incheon 20565, Republic of Korea.

http://dx.doi.org/10.1016/j.bmcl.2017.09.002
0960-894X/

The IC_{50} for compound **B**'s cytotoxic effect against MM cell lines with the highest DEPTOR expression was 0.8–2.5 μM. Thus, in a follow-up study to our previous work, we undertook a structure-activity relationship (SAR) study with the expectation of discovering chemically modified derivatives with enhanced efficacy. This report details our findings of this SAR study.

As previously described[4] we conducted a pilot screening of ~150,000 compounds from the NCI small molecule inhibitor library utilizing the yeast-2-hybrid screen, and identified four compounds ('hits') that specifically inhibited the DEPTOR-mTOR interaction (Fig. 1). Of these four, the first two compounds, NSC119055 and NSC119670, did not offer many opportunities for structural variation since they are quite simple structures. The third compound, NSC118305, presented several positions for variation but we were worried about the conjugated diene unit since such polyolefinic units might give a rise to non-selective toxicity. Indeed, this compound was toxic to normal hematopoietic colony forming cells, completely preventing colony formation when used as low as 0.5 μM (not shown). The final compound, NSC126405, was not toxic to colony formation (in concentrations as high as 10 μM) and yet demonstrated molecular efficacy (enhanced mTORC1 activity) and anti-MM cytotoxicity (MTT assays). Therefore we chose the final compound shown, NSC126405, which was called simply compound **B**, as the first compound to modify to try to improve its activity.

The possible modifications of all parts of compound **B** are shown in Fig. 2. Since it has been reported that unsubstituted analogues of **B**, those with the chlorines removed, are quite reactive nucleophiles,[5] likely due to the strong resonance structure which puts positive charge on the amino group and negative charge on the cyclopentadiene system, we decided to not pursue completely unsubstituted cyclopentadiene systems, hoping that more substituted ones would be more stable and less reactive. A series of compounds were prepared and tested for their biological activity in order to establish a comprehensive structure-activity relationship (SAR) for this series.

First we decided to modify the hydrazone unit and in particular to vary the substituents on the hydrazone amine nitrogen, namely the top part of compound **B** as shown in Fig. 2. The synthesis of these compounds was accomplished by several relatively easy routes (Scheme 1).[9] Thus condensation of commercially available hexachlorocyclopentadiene **1** with the selected hydrazine unit **2** in THF generally proceeded quite well. One could also use the HCl salts of the hydrazines and added base.[6] The best procedure was often to use the hydrazine HCl salt in pyridine as solvent. The desired compounds **3** were normally purified by flash column chromatography on silica gel and several could be recrystallized as well. The parent compound **B** was prepared by this route in 62% yield. We prepared some *N*-alkyl derivatives **3a–3c** and also used this route to prepare some *N*-aryl derivatives **3d–3l** by using either the alkyl hydrazines or the *N*-aminoanilines **2**, where R1 and/or R2 was an aryl group. The compounds **3a–3l** were generally quite deeply colored, e.g., dark orange or red.[7]

We next prepared several *N*-mono and di-acyl derivatives, **4a–4f** (Scheme 2).[8] The monoacyl compounds **4a** and **4c–4d** were synthesized by selective mono-acylation of the parent compound **B** with either acid anhydrides or acyl chlorides in the presence of base as shown. If **B** were treated with two equivalents of the acyl chloride and base, one obtained the diacylated derivatives **4b** and **4e–4f.** And we also prepared a few *N*-mono-carbamoyl derivatives **4g–4i,** which were prepared from **B** using di-*tert*-butyl dicarbonate or the corresponding alkyloxycarbonyl chloride.

Since there was some concern that compounds with the dichloroalkene unit might show some non-specific toxicity, we introduced a few cyclic and acyclic moieties in place of the tetrachlorocyclo-pentadiene ring system (Scheme 3).[9,10] We also

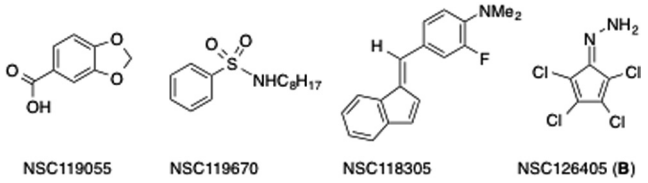

Fig. 1. Hit compounds from NCI inhibitor library.

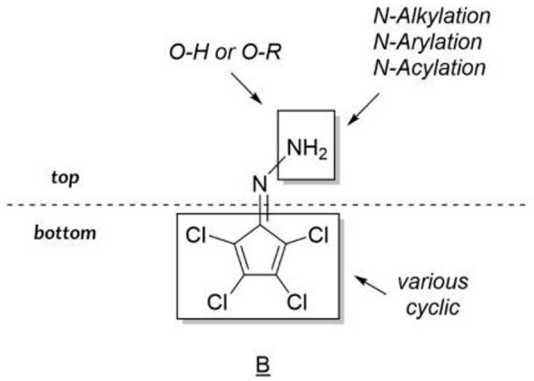

Fig. 2. Modification and SAR relationship of NSC126405 (**B**).

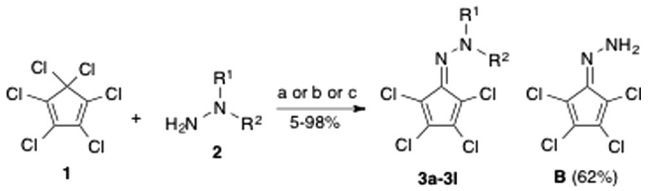

Scheme 1. Reagents and conditions: (a) **2** free form, THF, 22 °C; (b) **2** HCl salt, TEA, THF, 22 °C; (c) **2** HCl salt, pyr, 22 °C.

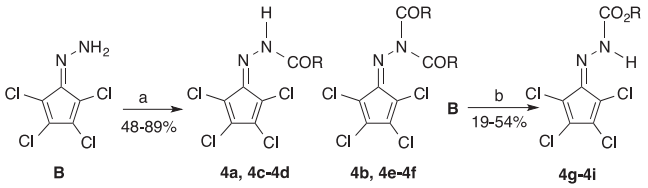

Scheme 2. Reagents and conditions: (a) 1 or 2 eq $(RCO)_2O$ or RCOCl, TEA, THF, 22 °C, 0.5–3 h; (b) $(ROCO)_2O$ or ROCOCl, pyr, DMAP, THF, 0 to 22 °C, 16–24 h.

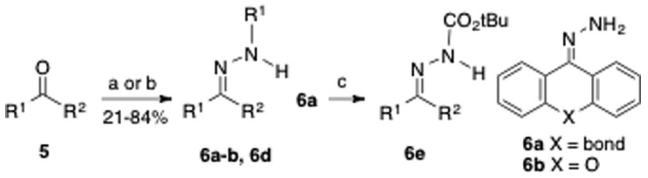

Scheme 3. Reagents and conditions: (a) N_2H_4, EtOH or triethylene glycol (TEG), reflux; (b) H_2N-NHR HCl, KOH, EtOH, reflux; (c) Di-*t*-butyl-dicarbonate, pyr, DMAP, THF, 0 to 22 °C, 3 h.

wanted to expand our substrate scope by further modifying the bottom part of the molecule. The hydrazones **6a**,[9] **6b,**[10] and **6d**, were prepared by reaction of the simple ketones, fluorenone and xanthone, **5**, R = H, R = (CH)4, with hydrazine or with hydrazine HCl salt and KOH in refluxing ethanol. The benzophenone hydra-

zine **6c** was commercially available. The *N*-Boc derivative **6e** was prepared from **6a** by treating the hydrazine with di-*tert*-butyl dicarbonate and pyridine and DMAP in THF.[11] The yields of the hydrazones **6a–6e** were generally quite good. We also prepared the unsubstituted hydrazones of indanone, cyclopentanone and acetophenone, but these compounds were unstable with respect to rearrangement to the dimeric azines.[12] Finally we prepared the oxime derivative **7a** and the dimethoxy analogue **7b**[13] from hexachlorocyclopentadiene **1** (Scheme 4).

The first set of analogues, **3a–3f** and **4a–4b**, were compared against the parent compound B in assays for mTORC1 activity. We used the 8226 cell line for these experiments as it demonstrates marked over-expression of DEPTOR.[1,3] As drugs that prevent binding of the mTOR inhibitor, DEPTOR, to mTOR, effective drugs should increase mTOR kinase activity. In mTORC1, mTOR phosphorylates the p70S6 kinase. Thus, we used Western blot to test for induction of p70 phosphorylation in this secondary screen. Compounds were tested at 0.5, 1, and 2 μM with 6 h *in vitro* exposure. Induction of p70 phosphorylation by all 8 derivatives was comparable to that of parent compound **B** when used at 1 or 2 μM except for the mono-benzoylated compound **4a** which was toxic and showed degradation of p70. However, at 0.5 μM, the three *N*-aryl compounds **3d–3f** and the dibenzoylated compound **4b** were more effective than the parent compound **B** for induction of p70 phosphorylation (selected immunoblot shown in Fig. 3A). In contrast, the *N*-alkyl compounds 3a–3b did not exhibit a significant increase of activity compared to compound **B**, while the *tert*-butyl compound **3c** showed only modest activity. Again, the mono-benzoylated compound **4a** was toxic with considerable cell death seen even at this low concentration (0.5 μM). Follow-up experiments on compound **4a** at lower concentrations which did not show toxicity (0.05–0.2 μM) demonstrated no enhancement of p70 phosphorylation suggesting compound **4a** was non-specifically toxic. A summary of the p70 phosphorylation data from 4 separate experiments where derivatives were used at 0.5 μM, is shown in Fig. 3B. These first 8 derivatives were also screened for cytotoxicity against the same 8226 MM cell line in 48 h MTT assays. The IC_{50}s for these assays are shown below the bar graphs in Fig. 3B and an example of one experiment is shown in Fig. 3C. In general, the analogues showed a correlation between the molecular effects (i.e., the ability to increase p70 phosphorylation) and their anti-MM cytotoxic effects. The four analogues (**4b**, **3d**, **3e** and **3f**) with enhanced molecular effects compared to the parent compound **B** also demonstrated lower IC_{50}s. In contrast, compounds **3a–3c**, which showed little or no enhancement of p70 phosphorylation compared to the parent compound **B**, also did not show enhanced anti-MM cytotoxicity. As mentioned above, compound **4a** was cytotoxic without effects on p70 phosphorylation; thus, its anti-MM effects were assumed to be non-specific.

On the basis of the initial result from the first set of analogues **3a–3f** and **4a–4b**, we designed and synthesized further analogues in four categories, and evaluated their molecular and anti-MM cytotoxic activities in p70 phosphorylation and MTT assays. P70 phosphorylation was measured in 8226 cells treated for 6 h. Since the parent compound **B** was consistently ineffective in inducing p70 phosphorylation following exposure of 8226 cells to 0.5 μM, we used 0.5 μM concentration to screen these additional derivatives for enhanced molecular activity. MTT (48 h) assays exploited 8226 cells as well as an additional DEPTOR-over-expressing MM cell line, MM1.S. In general, MM1.S cells are less sensitive than 8226 to the cytotoxic activity of the parent compound B (IC_{50} of 1.3 μM and 3.0 μM for 8226 and MM1.S, respectively). The structures and biological activity of all derivatives are shown in Tables 1–4, categorized by structural modification.

First since the three *N*-arylated compounds **3d–3f** showed promising results, we prepared more aryl derivatives having either

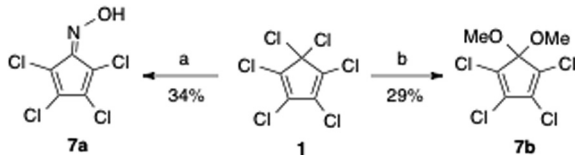

Scheme 4. Reagents and conditions: (1) Hydroxylamine HCl, KOH, MeOH, reflux, 8 h; (b) KOH, MeOH, 22 °C, 18 h.

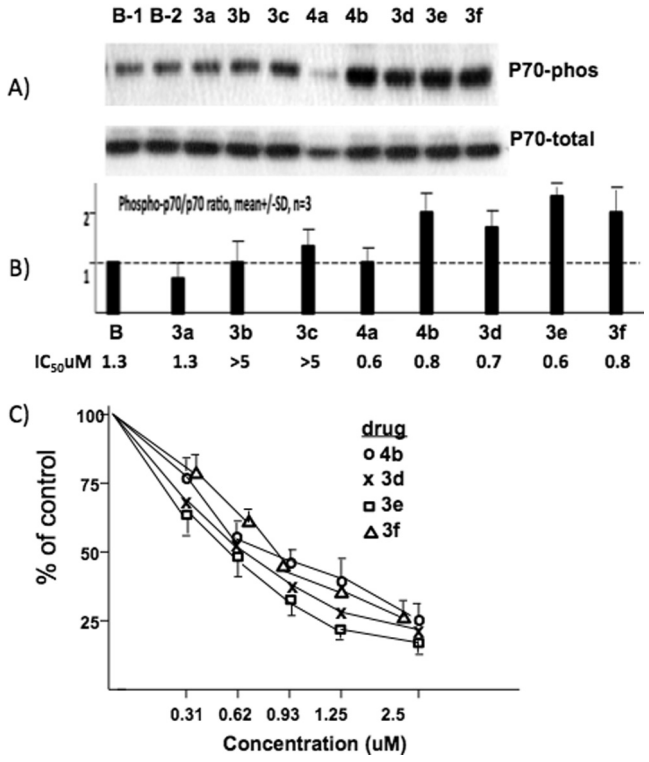

Fig. 3. A) 8226 cells exposed to drugs at 0.5 μM for 6 h, followed by immunoblot for expression of phosphorylated p70S6K, total p70 or actin. B-1 = compound **B** from NCI; B-2 = compound **B** synthesized at UCLA. B) Summary of p70 phosphorylation data from 4 separate experiments (n = 4) where derivatives were used at 0.5 μM, mean ± SD; IC50 (mean) from MTT cytotoxicity assays (n = 4) shown below bars. C) MTT cytotoxicity data (mean ± SD of triplicate samples) of four initially tested derivatives (**4b, 3d, 3e** and **3f**).

electron-withdrawing or electron-donating groups on the 3-position of phenyl ring **3g–3i** to examine the effect of phenyl substituents on the hydrazone in more detail. In Table 1, we present p70 phosphorylation and MTT assay results of compound **3a–3l**. The best activity was shown by the 3-trifluoromethylphenyl analogue **3g**, namely a 4-fold increase in p70 phosphorylation and an IC_{50} of 0.17 μM and 1.0 μM for the 8226 and MM1.S MM cell lines, respectively. The analogues having electron-donating group, **3h–3i,** did not show good activity. Generally the analogues with the more electron-withdrawing substituents showed the best activity, e.g., **3g** and **3k**. We also examined the effect of the position of the substituent. Although the 3-fluoro and 4-fluoro analogues, **3e** and **3k**, showed similar IC_{50} values in the 8226 and MM1.S cell lines, curiously the 4-fluoro analogue **3k** showed much better activity in the p70 phosphorylation assay, while the 2-fluoro analogue **3j** showed no activity. Finally the diphenyl analogue **3l** did not show any activity.

Next, we examined a series of analogues of the mono- and di-acyl derivatives **4a–4f** as well as some carbamate derivatives **4g–4i** (Table 2). The presumed non-specific toxicity of the mono-ben-

Table 1
p70 phosphorylation and cytotoxicity of alkyl and aryl analogues **3a–l**.

	R^1	R^2	p70 phosphorylation vs **B**[a]	MTT (IC_{50}, μM)	
				8226	MM1.S
B	H	H	1.0	1.3	3.0
3a	CH_3	CH_3	NI	>3	>3
3b	C_6H_{11}	H	NI	>3	>3
3c	$C(CH_3)_3$	H	NI	>3	>3
3d	C_6H_5	H	1.8	0.6	2.0
3e	3-FC_6H_4	H	2.2	0.5	1.5
3f	3,5-$Cl_2C_6H_3$	H	1.9	0.8	2.0
3g	3-$CF_3C_6H_4$	H	4.0	0.17	1.0
3h	3-MeC_6H_4	H	NI	2.0	>3
3i	3-$MeOC_6H_4$	H	NI	>3	>3
3j	2-FC_6H_4	H	NI	>3	>3
3k	4-FC_6H_4	H	5.0	0.7	1.3
3l	C_6H_5	C_6H_5	NI	>3	>3

[a] Fold increase, measured at 0.5 μM. NI = no increase.

Table 2
p70 Phosphorylation and cytotoxicity of acyl and carbamate derivatives **4a–4i.**

Compd	R	p70 phosphorylation vs **B**[a]	MTT (IC_{50}, μM)	
			8226	MM1.S
B		1.0	1.3	3.0
4a	C_6H_5	NI	0.6	0.8
4b	C_6H_5	2.0	0.8	2.0
4c	CH_3	NI	1.0	ND
4d	$C(CH_3)_3$	7.0	0.12	2.0
4e	4-FC_6H_4	5.0	0.25	0.3
4f	4-MeC_6H_4	2.5	0.5	0.5
4g	$C(CH_3)_3$	6.0	0.1	0.6
4h	$CH_2C{\equiv}CH$	1.5	0.8	ND
4i	$C(CH_3)_2C{\equiv}CH$	1.2	>5	ND

[a] Fold increase, measured at 0.5 μM; ND, not determined; NI, no increase.

Table 3
p70 Phosphorylation, cytotoxicity and apoptosis of derivatives **6a–6e.**

	R^1	R^2	R	p70 phosphorylation vs **B**[a]	MTT (IC_{50}, μM)	
					8226	MM1.S
B	2,3,4,5-Cl_4C_5		H	1.0	1.5	3.0
6a	9-Fluorenyl		H	NI	>5	ND
6b	9-Xanthyl		H	NI	>5	>5
6c	Ph	Ph	H	NI	>5	>5
6d	9-Fluorenyl		3-FC_6H_4	NI	>5	>5
6e	9-Fluorenyl		*t*-Boc	NI	>5	>5

[a] Fold increase, measured at 0.5 μM; ND, not determined; NI, no increase.

Table 4
p70 Phosphorylation, cytotoxicity and apoptosis of derivatives **7a–7b.**

	structure	p70 phosphorylation vs **B**[a]	MTT (IC_{50}, μM)	
			8226	MM1.S
B	hydrazone	1.0	1.5	3.0
7a	oxime	NI	>5	ND
7b	dimethoxy	NI	>5	ND

[a] Fold increase, measured at 0.5 μM; ND, not determined; NI, no increase.

zoylated analogue **4a** was again shown by the MTT assays with IC_{50} values of 0.6 and 0.8 μM for 8226 and MM1.S, respectively. The mono-acetylated analogue **4c** also showed no increase of p70 phosphorylation at 0.5 μM compared to compound **B** treatment, and similar cytotoxicity (vs drug **B**) to 8226 cells. On the other hand, the mono-pivaloylated analogue **4d** showed a substantial 7-fold increase in p70 phosphorylation which correlated nicely with lowered IC_{50} values for both cell lines in the MTT assays, 0.12 μM and 2.0 μM for 8226 and MM1.S, respectively.

Since the *N*-dibenzoylated compound **4b** was quite promising in the initial testing, we then prepared two additional dibenzoylated compounds having different substituents on the 4-position of the phenyl ring. As expected, both compounds **4e** and **4f** showed good results for p70 phosphorylation and MTT assays. Moreover, in line with the results of the aryl derivatives, compound **4e** having

an electron-withdrawing substituent on the 4-position showed even better results than the other two diacyl derivatives. We also prepared and examined the carbamate derivatives **4g–4i**. The *tert*-butyloxy-carbonyl analogue **4g** showed a substantial 6-fold increase in p70 phosphorylation and also enhanced cytotoxicity, 0.1 μM and 0.6 μM IC_{50} for 8226 and MM1.S, respectively. The other carbamate derivatives **4h** and **4i** having a terminal acetylene were prepared for the possible further investigation of biotin protein labeling by click chemistry, but these compounds showed a minimal increase in mTORC1 activation. Only the simple propargyl compound **4h** showed some cytotoxicity in the MTT assay.

It is perhaps interesting to compare the three analogues having a *tert*-butyl unit, namely the alkyl analogue, **3c**, the acyl analogue **4d**, and the carbamate **4g**. The alkyl analogue **3c** showed the least activity in p70 phosphorylation, while the pivaloyl (*tert*-butylcarbonyl) analogue **4d** and the *t*-Boc (*tert*-butyloxycarbonyl) analogue **4g** showed very good activities in both p70 phosphorylation and MTT assay.

Next we examined the derivatives **6a-6e** having cyclic and acyclic moieties other than the tetrachlorocyclopentadiene ring system (Table 3). We left unchanged the unsubstituted hydrazine as the top unit and modified the bottom part to 9-fluorenyl **6a**, 9-xanthyl **6b** and benzophenone **6c**. However these new analogues did not show any improvement in both the p70 phosphorylation and the MTT assay. Since the 3-fluorophenyl (**3e**) and *t*-Boc carbamate (**4g**) analogues showed enhanced biological activities reasons that are still unclear. Finally, we examined the oxime and dimethoxy derivatives, **7a** and **7b**, and they both showed poor activity in the p70 phosphorylation and the MTT cytotoxicity assay (Table 4).

All the derivatives in each category showed a rough correlation between the derivatives that were successful molecularly, namely able to increase p70 phosphorylation at 0.5 μM, and were effective cytotoxic compounds. Of the nine molecules (**3d**, **3e**, **3f**, **3g**, **3k**, **4b**, **4d**, **4e** and **4g**) active in the p70 phosphorylation assay (≥1.8-fold increase compared to compound **B** at 0.5 μM), all had enhanced cytotoxic effects (i.e., lower IC_{50}) compared to the parent **B**. Of the many compounds without molecular efficacy (i.e., <1.8-fold increase in p70 phosphorylation), only two – **4a** and **4h** – demonstrated enhanced cytotoxic effects, which were presumably non-specific.

From these screening experiments, we identified analogues **3g**, **3k**, **4d**, **4e** and **4g** as being the most active compounds in the p70 phosphorylation assay. These were then studied in more detail. As shown in Fig. 4A and B, although inducing comparable amounts of p70 phosphorylation at 1 μM, when compared to parent compound **B** at lower concentrations, these biochemically modified compounds were significantly more effective as low as 0.25 μM. An additional molecular effect of either DEPTOR knockdown or parent compound **B** is an upregulation of p21 expression,[3,4] believed to result from decreased mTORC1-dependent expression of p21-targeting miRNAs.[3] Upregulated expression of p21 contributes to the anti-MM cytotoxicity of DEPTOR targeting.[3] As shown in Fig. 4C, some of these derivatives with enhanced mTORC1 activation compared to parent compound **B** also demonstrated enhanced p21 expression, further strengthening the notion that their biochemical modifications allow more efficacious DEPTOR targeting. This was clearly shown for **4d**, **4e**, **4g**, and **3g**. Fig. 4D also demonstrates the enhanced anti-MM cytotoxicity of these agents in 8226 MTT assays. We also tested the ability of these drugs to enhance apoptosis in 8226 cells and, as shown in Fig. 4E, their apoptosis activity was enhanced compared to parent compound **B**.

To compare anti-myeloma efficacy to non-specific toxicity, we compared each of these 5 active derivatives to compound **B** in their ability to inhibit survival of 8226 MM cells versus normal peripheral blood lymphocytes (PBLs). In head-to-head experiments, IC_{50} values for each target were calculated and compared. As shown in Fig. 5A, although each of the derivatives demonstrated significantly reduced IC_{50} values for the MM cells compared to compound **B**, they also showed variably enhanced toxicity to PBLs. However, three of the derivatives, **3g**, **3k** and **4g**, showed significantly greater therapeutic indices (TI) compared to compound **B**. To further support the fact that the ability of these three active derivatives (**3g**, **3k** and **4g**) to induce MM cell death was specifically related to their successful interference of DEPTOR/mTOR binding and mTORC1 activation, we performed co- immunoprecipitation experiments. Compound **B** prevents DEPTOR/mTOR binding in MM cells when used at 1 μM but at 0.5 μM it is ineffective (Fig. 5B). However, all three derivatives with enhanced TIs prevented DEPTOR/mTOR binding when used at 0.5 μM (Fig. 5C). To test if drug cytotoxicity was due to mTORC1 activation, we assessed derivatives for their anti-MM cytotoxicity in isogenic lines with RAPTOR knockdown. Fig. 5D demonstrates the inhibitory effects of RAPTOR knockdown on mTORC1 activation. As shown in Fig. 5E, MTT cytotoxicity assays demonstrate a significantly decreased cytotoxicity induced by all three derivatives when tested against the RAPTOR-silenced MM cells. This indicates mTORC1 activation contributes to cytotoxicity.

Although RAPTOR knockdown, by itself, had no discernable cytotoxic effects (i.e., normal viability, (not shown)), it was always possible that RAPTOR silencing altered the growth characteristics of the cells. Thus, we independently tested the effects of pp242, an mTOR kinase inhibitor, which would also theoretically prevent mTORC1 activation, on the cytotoxic effects of drugs **3g** and **4g**. As shown in Suppl Fig. 1, MTT cytotoxicity and apoptosis induction was significantly decreased when pp242 was added to our compounds in a concentration that prevented mTORC1 activation. Thus, in two independent strategies where mTORC1 activation was prevented (RAPTOR knockdown and pp242 exposure), anti-myeloma cytotoxicity was abated, confirming that mTORC1 activation participates in the effectiveness of our compounds.

Blocking the interaction between mTOR and DEPTOR (see Fig. 5C) should enhance kinase activity of both mTORC1 and mTORC2. To further investigate these downstream molecular effects for two of the most promising anti-myeloma derivatives (compounds **4g** and **3g**), we performed additional Western blot experiments (Supplemental Fig. 2). The previous experiments demonstrated an increase in p70 phosphorylation indicating the expected activation of mTORC1. Both compounds also induced phosphorylation of 4E-BP1 (Supplemental Fig. 2), an additional substrate of mTORC1. Phosphorylation of S6 was also increased indicating not only increased phosphorylation of p70S6kinase but increased kinase activity as well. These data confirm the activation of mTORC1 in drug-treated myeloma cells. We also assayed mTORC2 activity by analysis of AKT serine 473 phosphorylation, as serine 473 is a substrate of mTORC2. As shown in Supplemental Fig. 2, exposure to both compounds resulted in enhanced S473 phosphorylation. In addition, SGK, a direct substrate of AKT kinase activity, was increased in its phosphorylation. These data strongly support activation of mTORC2 as well as mTORC1 following a block of the DEPTOR-mTOR interaction. It is remarkable that, even in the presence of enhanced AKTS473 phosphorylation and AKT activity (i.e., SGK phosphorylation), these compounds are so significantly cytotoxic to myeloma cells.

When DEPTOR is silenced by shRNA and mTORC1 is upregulated, activated TORC1 results in feedback downregulation of the IGF/IRS-1/PI3-K/PDK1 pathway.[1,3] This results in decreased phosphorylation of AKT on serine 308 (a PDK1 substrate). A comparable effect is seen in myeloma cells treated with **3g** or **4g** (Supplemental Fig. 2), supporting the notion that, similar to effects of DEPTOR gene silencing, this negative feedback pathway is impacted. The difference between our anti-myeloma drugs and gene silencing is

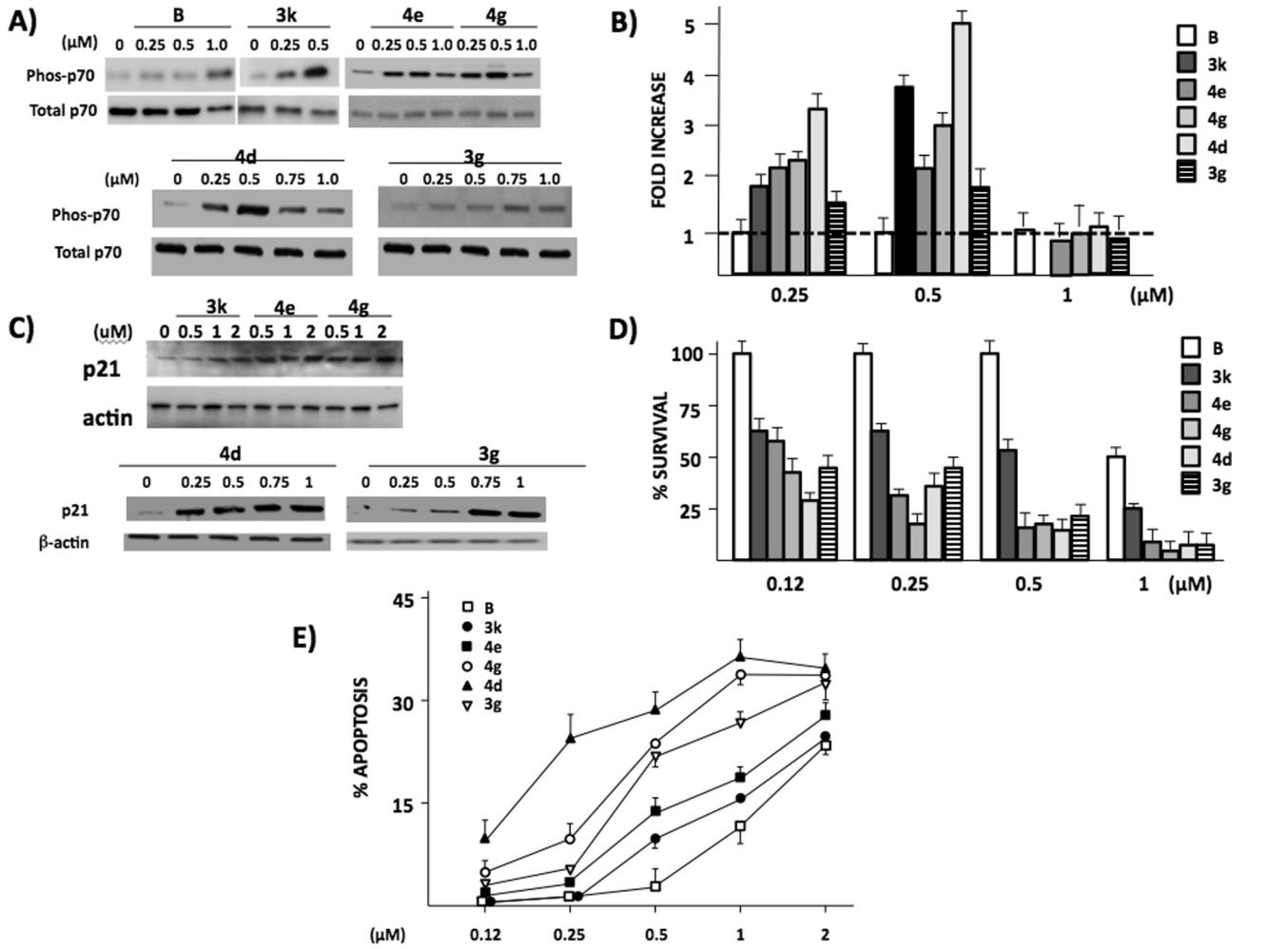

Fig. 4. A) Representative experiment of p70 phosphorylation w/ increasing concentrations of derivatives vs compound **B** (exposure 6 h); B) Summary of p70 phosphorylation data (mean ± SD, n = 4) shown as fold increase vs compound **B** (compound **B** kept at '1') of densitometric ratio of phospho-p70/total p70 after exposure to derivatives for 6 h; C) Upregulated p21 expression due to derivatives. D) MTT assays of all derivatives vs compound **B** (48 h assay), mean ± SD, n = 4; E) % apoptosis (mean ± SD, n = 4) at 48 h after exposure to different derivatives. In all immunoblot experiments, untreated control groups (μM = 0) contain an equal amount of DMSO.

the effects on AKT S473 phosphorylation where our compounds increase activation and DEPTOR knockdown decreases activation. It is likely that the resulting increase in mTORC2 activity in drug-treated cells (due to the prevention of DEPTOR-mTOR binding) overcomes any inhibitory effect on the PI3-K/PDK1/AKT pathway. Nevertheless, It is evident that our therapeutic compounds do not kill myeloma cells by down-regulating the prosurvival effects of AKT as suggested by Peterson[1] in DEPTOR-silenced cells. This is consistent with our previous work[4] on drug **B**, the initial 'hit' in the yeast screen.

We also considered an outside possibility that the most effective agent, compound **3g**, was inducing mTOR kinase activity independent of DEPTOR. Enhanced kinase activity with phosphorylation of DEPTOR, by itself, could theoretically prevent mTOR-DEPTOR binding (explaining the co-IP results) and induce p70 phosphorylation. To test this, we compared the effect of drug **3g** on DEPTOR-silenced cells. As expected (Supplemental Fig. 3), DEPTOR knockout by itself (achieved by shRNA) resulted in enhanced P70 phosphorylation (6× fold increase). However, drug **3g** was incapable of further mTORC1 activation in these cells while inducing significant p70 phosphorylation (4× fold increase) in control cells (transfected with shScramble lentivirus). Thus, the activation of mTORC1 in drug **3g**-treated cells is dependent on the presence of DEPTOR.

We have initiated *in vivo* toxicity studies with the most promising derivative, **3g**. Immunodeficient mice were challenged subcutaneously with 8226 cells (as described in ref 4) and, when tumors reached 500 mm^3, daily treatment with 20 mg/kg of compound **B** or drug **3g** was initiated. The aim of the experiment was to test short-term toxicity of drug **3g** on hematopoiesis with a dose of drug that demonstrated anti-MM efficacy. Although a more thorough dose-dependent toxicity vs efficacy study is planned in the future, this initial experiment with analogue **3g** indicates an enhanced anti-myeloma effect in vivo vs drug **B**. As shown in Supplemental Fig. 4, compound **3g** had no toxic effects on RBC, WBC or platelet levels but it induced a significantly more rapid tumor cytoreductive response compared to drug **B** which was evident by day +3 of treatment.

Although activating mTORC1 and mTORC2, the compounds described in this study have therapeutic potential in multiple myeloma. However, in other tumor models where DEPTOR expression is low and mTOR activity is high, these therapeutics may be less promising and even, possibly, harmful, due to possible stimulation of tumor cell proliferation. Nevertheless, they have promise in myeloma. Thus, we have prepared a series of analogues of the initial hit, NSC126405, compound **B**, from our high-throughput screen. Several derivatives of the parent compound **B** showed promising activity with *N*-aryl, *N*-mono and diacyl and *N*-car-

A) IC_{50} (μM)

Compd	8226	PBLs	TI
B	1.4	20	14.3
3k	0.6	20	33
4e	0.2	2.0	10
4g	0.11	5	45.5
4d	0.09	1.25	14
3g	0.11	15	136

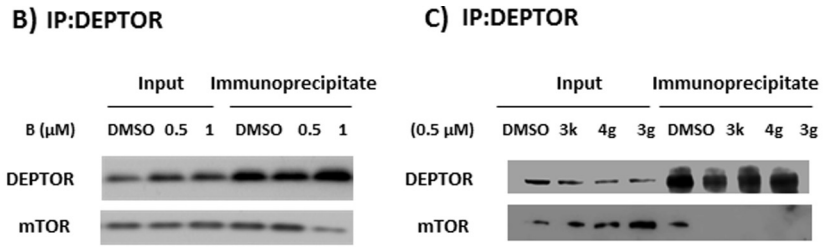

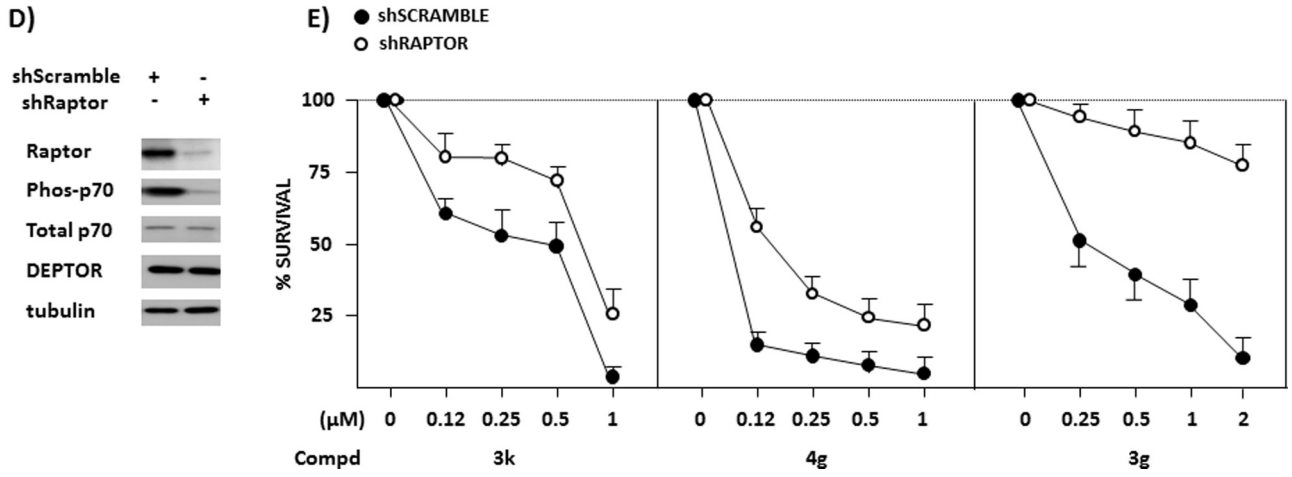

Fig. 5. A) IC_{50}s of drug **B** and derivatives against 8226 MM cells or PBLs (48 h assays, results are means of 5 separate experiments). Therapeutic indices (TIs) calculated as IC_{50} PBLs/IC_{50} for 8226 cells; B) 8226 cells treated with DMSO or drug **B** (6 h) followed by immunoprecipitation of DEPTOR and precipitate then immunoblotted for DEPTOR or bound mTOR. C) 8226 cells treated with DMSO or 0.5 μM of derivatives (6 h) followed by similar co-immunoprecipitation assay. D) 8226 cells infected with lentivirus expressing either shRAPTOR or control shSCRAMBLE followed by immunoblot assay for RAPTOR, phosphorylated p70, total p70, DEPTOR or tubulin; E) MM cells expressing either shSCRAMBLE or shRAPTOR incubated with increasing concentrations of derivatives, followed by MTT assay (48 h). Cytotoxicity (i.e., decreased cell survival) induced in RAPTOR-silenced cells was significantly reduced ($p < 0.05$) compared to control shSCRAMBLE cells.

bamoyl analogues being the most promising. From these studies, we have identified five new leads, **3g**, **3k**, **4d**, **4e** and **4g** (Fig. 6). The ability of these more efficacious derivatives to inhibit mTOR-DEPTOR binding in MM cells when used at lower concentrations (vs drug **B**) was demonstrated by co-immunoprecipitation studies. Further support for their specificity is the finding that their enhanced cytotoxicity to MM cells is significantly prevented by mTORC1 inactivation. This indicates that, similar to drug **B**, their acute activation of mTORC1 subsequent to DEPTOR targeting participates in the injury to MM cells. Our previous work demonstrates direct binding of drug **B** to recombinant DEPTOR.[4] One possible explanation for enhanced activity of the derivatives is that their binding to DEPTOR may be quantitatively or qualitatively different than that of drug **B**. Further research into the mechanism of action and selectivity of these compounds, as well as additional analogues, is currently underway.

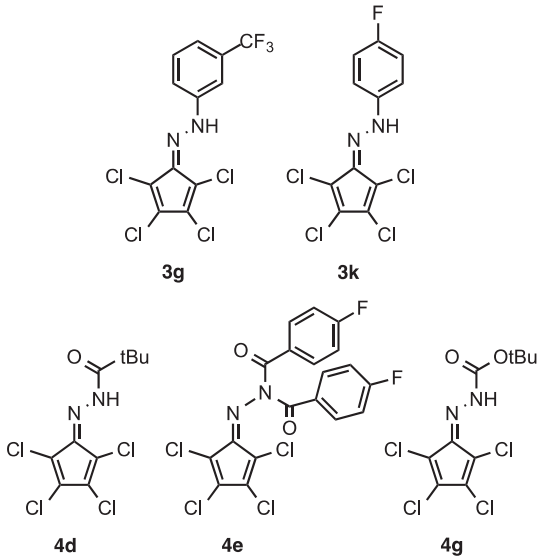

Fig. 6. Most active analogues.

Experimental

Chemistry

General methods

All reactions were carried out under open-air condition unless otherwise specified. Tetrahydrofuran (THF) was distilled from benzophenone ketyl radical under an argon atmosphere. Methanol, dichloromethane (DCM) and triethylamine (TEA) were distilled from calcium hydride under an argon atmosphere. Hexachlorocyclopentadiene was purchased from Chemieliva Pharmaceutical Co. in China and various hydrazines were purchased from Sigma-Aldrich, Alfa Aesar and TCI in ≥95% purity, all other solvents or reagents were purified according to literature procedures if neces-

sary. ^{1}H NMR spectra were recorded on Bruker spectrometers at 500 MHz and are reported relative to deuterated solvent signals ($CHCl_3$ δ 7.26; DMSO δ 2.48 ppm). Data for ^{1}H NMR spectra are reported as follows: chemical shift (δ ppm), multiplicity, coupling constant (Hz) and integration. Splitting patterns are designated as follows: s, singlet; d, doublet; t, triplet; q, quartet; dd, doublet of doublets; dt, doublet of triplets; td, triplet of doublets; tt, triplet of triplets; qd, quartet of doublets; qt, quartet of triplets; m, multiplet; and br, broad. ^{13}C NMR spectra were recorded on Bruker Spectrometers at 125 MHz and are reported relative to deuterated solvent signals ($CHCl_3$ δ 77.0; DMSO δ 40.0 ppm). ^{19}F NMR spectra were recorded on Bruker Spectrometers at 376.3 MHz and are reported relative to external Freon-113 in benzene (δ −73.75 ppm). Data for ^{13}C and ^{19}F NMR spectra are reported in terms of chemical shift. The chemical shifts are reported in parts per million (ppm, δ). Melting points were obtained using Buchi B-545 melting point apparatus and are uncorrected. The reactions were monitored with a silica gel TLC plate under UV light (254 and 365 nm) followed by visualization with a ninhydrin or phosphomolybdic acid staining solution. Column chromatography was performed on silica gel 60, 230–400 mesh. DART-HRMS spectra were collected on a Thermo Exactive Plus MSD (Thermo Scientific) equipped with an ID-CUBE ion source and a Vapur Interface (IonSense). Both the source and MSD were controlled by Excalibur, version 3.0. The purity of the compounds was assayed by high field proton and carbon NMR and was ≥95%.

Synthetic procedures and characterization data

(Perchlorocyclopenta-2,4-dien-1-ylidene)hydrazine (B). To a solution of hexachlorocyclopentadiene (1.6 mL, 10.0 mmol, 1.0 eq) in tetrahydrofuran (50 mL) was added hydrazine monohydrate (1.45 mL, 30.0 mmol, 3.0 eq) dropwise at 0 °C. The reaction mixture was stirred for 10 min at room temperature and then concentrated in vacuo. The residue was purified by flash column chromatography over silica gel (hexane/ethyl acetate, 10:1, v/v) to afford the desired product **B** (1.44 g, 62%) as red brown solid: Rf = 0.4 (hexane/ethyl acetate, 5:1, v/v); mp 187–189 °C; ^{1}H NMR (DMSO-d_6, 500 MHz) δ 10.67 (d, J = 3.2 Hz, 1H), 9.93 (d, J = 3.6 Hz, 1H); ^{1}H NMR ($CDCl_3$, 500 MHz) δ 8.09 (br, 2H); ^{13}C NMR (DMSO-d_6, 125 MHz) δ 129.2, 125.6, 119.8, 118.2, 104.2; ^{13}C NMR ($CDCl_3$, 125 MHz) δ 132.7, 131.2, 124.6, 119.5, 105.8 ppm; DART-HRMS found 230.88672 $[M+H]^+$, calcd for $C_5H_3Cl_4N_2$ 230.90448.

Representative procedure for synthesis of alkyl and aryl hydrazones

*Method A. 1,1-Dimethyl-2-(perchlorocyclopenta-2,4-dien-1-ylidene)hydrazine (**3a**).* To a solution of hexachlorocyclopentadiene (0.16 mL, 1.0 mmol, 1.0 eq) in tetrahydrofuran (10 mL) was added unsym-dimethyl-hydrazine (0.23 mL, 3.0 mmol, 3.0 eq) dropwise at 0 °C. The reaction mixture was stirred for 3 h at room temperature and then concentrated in vacuo. The residue was diluted with ethyl acetate (80 mL) and washed with water (2 × 20 mL) and brine (20 mL). The organic layer was dried with MgSO4, filtered and concentrated in vacuo. The residue was purified by flash column chromatography over silica gel (hexane/ethyl acetate, 10:1, v/v) to afford the desired product **3a** (254 mg, 98%) as dark brown solid: Rf = 0.45 (hexane/ethyl acetate, 3:1, v/v); mp 69–71 °C; ^{1}H NMR ($CDCl_3$, 500 MHz) δ 3.59 (s, 6H); ^{13}C NMR ($CDCl_3$, 125 MHz) δ 129.5, 128.4, 121.8, 119.4, 103.0, 50.5 ppm; DART-HRMS found 258.93448 $[M+H]^+$, calcd for $C_7H_7Cl_4N_2$ 258.93634.

*1-(Perchlorocyclopenta-2,4-dien-1-ylidene)-2-phenylhydrazine (**3d**).* Dark brown solid (94% yield): Rf = 0.65 (hexane/ethyl acetate, 3:1, v/v); mp 130–131 °C; ^{1}H NMR ($CDCl_3$, 500 MHz) δ 10.7 (s, 1H), 7.40 (td, J = 7.5, 1.5 Hz, 2H), 7.34 (dd, J = 9.0, 1.0 Hz, 2H), 7.15 (tt, J = 7.5, 1.0 Hz, 1H); ^{13}C NMR ($CDCl_3$, 125 MHz) δ 141.4, 130.94, 130.91, 129.7, 124.9, 123.9, 119.4, 115.1, 104.9 ppm; DART-HRMS found 306.91754 $[M+H]^+$, calcd for $C_{11}H_7Cl_4N_2$ 306.93634.

*1-(Perchlorocyclopenta-2,4-dien-1-ylidene)-2-(3-(trifluoromethyl) phenyl)hydrazine (**3g**).* Red brown solid (46% yield): Rf = 0.45 (hexane/ethyl acetate, 10:1, v/v); mp 146–148 °C; ^{1}H NMR ($CDCl_3$, 500 MHz) δ 10.69 (s, 1H), 7.53–7.52 (m, 3H), 7.38 (d, J = 5.0 Hz, 1H); ^{13}C NMR ($CDCl_3$, 125 MHz) δ 142.0, 132.2 (q, J_{CF} = 32.0 Hz, 1C), 130.3, 126.9, 125.2, 124.8, 122.6, 121.1 (q, J_{CF} = 3.5 Hz, 1C), 119.8, 117.9, 111.7 (q, J_{CF} = 3.8 Hz, 1C), 105.4; ^{19}F NMR ($CDCl_3$, 376 MHz, ^{1}H-dc) δ -62.90 ppm; DART-HRMS found 374.90492 $[M+H]^+$, calcd for $C_{12}H_6Cl_4F_3N_2$ 374.92372.

*1-(Perchlorocyclopenta-2,4-dien-1-ylidene)-2-(m-tolyl)hydrazine (**3h**).* Red brown solid (32% yield): Rf = 0.65 (hexane/ethyl acetate, 5:1, v/v); mp 139–141 °C; ^{1}H NMR (DMSO-d_6, 500 MHz) δ 11.55 (s, 1H), 7.36 (s, 1H), 7.34 (d, J = 9.0 Hz, 1H), 7.30 (t, J = 7.5 Hz, 1H), 7.00 (d, J = 7.5 Hz, 1H); ^{13}C NMR ($CDCl_3$, 125 MHz) δ 141.4, 139.8, 130.8, 130.7, 129.5, 125.9, 123.7, 119.3, 115.6, 112.3, 104.8, 21.5 ppm; DART-HRMS found 320.93277 $[M+H]^+$, calcd for $C_{12}H_8Cl_4N_2$ 320.95199.

*Method B. 1-Cyclohexyl-2-(perchlorocyclopenta-2,4-dien-1-ylidene)hydrazine (**3b**).* To a suspension of cyclohexylhydrazine HCl (527 mg, 3.5 mmol, 3.5 eq) in tetrahydrofuran (5 mL) was added triethylamine (0.49 mL, 3.5 mmol, 3.5 eq) and the mixture was stirred for 0.5 h. To a solution of hexachlorocyclopentadiene (0.16 mL, 1.0 mmol, 1.0 eq) in tetrahydrofuran (5 mL) was added the previously generated free form of cyclohexyl-hydrazine through filtration at room temperature. The reaction mixture was stirred for 12 h at room temperature and then concentrated in vacuo. The residue was diluted with ethyl acetate (80 mL) and washed with water (2 × 20 mL) and brine (20 mL). The organic layer was dried with MgSO4, filtered and concentrated in vacuo. The residue was purified by flash column chromatography over silica gel (hexane only) to afford the desired product **3b** (60 mg, 19%) as red brown solid: Rf = 0.5 (hexane only); mp 79–81 °C; ^{1}H NMR (DMSO-d_6, 500 MHz) δ 10.36 (d, J = 4.0 Hz, 1H), 3.61–3.56 (m, 1H), 1.93–1.89 (m, 2H), 1.76–1.72 (m, 2H), 1.60–1.56 (m, 1H), 1.53 (qd, J = 12.5, 3.5 Hz, 2H), 1.31 (qt, J = 12.5, 3.5 Hz, 2H), 1.13 (qt, J = 12.5, 3.5 Hz, 1H); ^{13}C NMR (DMSO-d_6, 125 MHz) δ 127.3, 124.6, 118.7, 117.2, 103.5, 61.4, 31.6, 25.3, 24.7 ppm; DART-HRMS found 312.96460 $[M+H]^+$, calcd for $C_{11}H_{13}Cl_4N_2$ 312.98329.

*1-(tert-Butyl)-2-(perchlorocyclopenta-2,4-dien-1-ylidene)hydrazine (**3c**).* Red solid (5% yield): Rf = 0.4 (hexane only); mp 80–82 °C; ^{1}H NMR (DMSO-d_6, 500 MHz) δ 9.98 (s, 1H), 1.34 (s, 9H); ^{13}C NMR ($CDCl_3$, 125 MHz) δ 127.3, 125.1, 119.1, 117.3, 103.9, 59.2, 28.2 ppm; DART-HRMS found 286.96594 $[M+H]^+$, calcd for $C_9H_{11}Cl_4N_2$ 286.96764.

*1-(3,5-dichlorophenyl)-2-(perchlorocyclopenta-2,4-dien-1-ylidene)hydrazine (**3f**).* Brown solid (16% yield): Rf = 0.6 (hexane/ethyl acetate, 5:1, v/v); mp 188–190 °C; ^{1}H NMR ($CDCl_3$, 500 MHz) δ 10.52 (s, 1H), 7.22 (d, J = 2.0 Hz, 2H), 7.10 (t, J = 2.0 Hz, 1H; ^{13}C NMR ($CDCl_3$, 125 MHz) δ 143.3, 136.2, 133.0, 132.7, 125.7, 124.3, 119.9, 113.4, 105.6 ppm; DART-HRMS found 374.83957 $[M+H]^+$, calcd for $C_{11}H_5Cl_4N_2$ 374.85839.

*Method C. 1-(3-Fluorophenyl)-2-(perchlorocyclopenta-2,4-dien-1-ylidene)hydrazine (**3e**).* To a solution of hexachlorocyclopentadiene (0.16 mL, 1.0 mmol, 1.0 eq) in pyridine (5 mL) was added 3-fluorophenyl hydrazine HCl (244 mg, 1.5 mmol, 1.5 eq) at room temperature. The reaction mixture was stirred for 12 h at room temperature and then concentrated in vacuo. The residue was diluted with ethyl acetate (80 mL) and washed with water (2 × 20 mL) and brine (20 mL). The organic layer was dried with $MgSO_4$, filtered and concentrated in vacuo. The residue was purified by flash column chromatography over silica gel (hexane only) to afford the desired product **3e** (212 mg, 65%) as brown solid: Rf = 0.6 (hexane/ethyl acetate, 5:1, v/v); mp 134–136 °C; ^{1}H NMR ($CDCl_3$, 500 MHz) δ 10.63 (s, 1H), 7.33 (dt, J = 6.5, 8.5 Hz, 1H),

7.15 (dt, J = 10.0, 2.0 Hz, 1H), 7.01 (dd, J = 8.0, 1.5 Hz, 1H), 6.83 (td, J = 8.0, 1.5 Hz, 1H); ^{13}C NMR ($CDCl_3$, 125 MHz) δ 163.8 (d, J_{CF} = 245.3 Hz, 1C), 143.2 (d, J_{CF} = 10.4 Hz, 1C), 131.9, 131.7, 131.0 (d, J_{CF} = 9.4 Hz, 1C), 124.8, 119.7, 1115. (d, J_{CF} = 21.5 Hz, 1C), 110.7 (d, J_{CF} = 2.9 Hz, 1C), 105.3, 102.3 (d, J_{CF} = 26.8 Hz, 1C); ^{19}F NMR ($CDCl_3$, 376 MHz, ^{1}H-dc) δ −110.42 ppm; DART-HRMS found 324.90814 $[M+H]^+$, calcd for $C_{11}H_6Cl_4FN_2$ 324.92691.

*1-(3-Methoxyphenyl)-2-(perchlorocyclopenta-2,4-dien-1-ylidene) hydrazine (**3i**).* Red brown solid (50% yield): Rf = 0.4 (hexane/ethyl acetate, 10:1, v/v); mp 123–125 °C; ^{1}H NMR ($CDCl_3$, 500 MHz) δ 10.66 (s, 1H), 7.27 (t, J = 8.0 Hz, 1H), 6.96 (s, 1H), 6.84 (dd, J = 8.0, 1.0 Hz, 1H), 6.69 (dd, J = 8.0, 1.5 Hz, 1H), 3.85 (s, 3H); ^{13}C NMR ($CDCl_3$, 125 MHz) δ 161.0, 142.7, 131.0, 130.9, 130.5, 124.0, 119.4, 110.7, 107.7, 105.0, 100.6, 55.4 ppm; DART-HRMS found 336.92801 $[M+H]^+$, calcd for $C_{12}H_8Cl_4N_2O$ 336.94690.

*1-(2-Fluorophenyl)-2-(perchlorocyclopenta-2,4-dien-1-ylidene) hydrazine (**3j**).* Red brown solid (52% yield): Rf = 0.6 (hexane/ethyl acetate, 20:1, v/v); mp 120–122 °C; ^{1}H NMR (DMSO-d_6, 500 MHz) δ 11.16 (s, 1H), 7.65 (t, J = 8.0 Hz, 1H), 7.36 (dd, J = 10.0 Hz, 1H), 7.29 (t, J = 7.5 Hz, 1H), 7.20 (dd, J = 12.5, 6.0 Hz, 1H), 3.32 (s, 3H); ^{13}C NMR ($CDCl_3$, 125 MHz) δ 151.1 (d, J_{CF} = 242.4 Hz, 1C), 132.7, 131.8, 130.1, (d, J_{CF} = 8.4 Hz, 1C), 125.3 (d, J_{CF} = 3.5 Hz, 1C), 124.8, 124.6 (d, J_{CF} = 7.3 Hz, 1C), 119.5, 115.6, 115.5 (d, J_{CF} = 17.4 Hz, 1C), 105.6; ^{19}F NMR ($CDCl_3$, 376 MHz, ^{1}H-dc) δ -135.16 ppm; DART-HRMS found 324.90775 $[M+H]^+$, calcd for $C_{11}H_6Cl_4FN_2$ 324.92691.

*1-(4-Fluorophenyl)-2-(perchlorocyclopenta-2,4-dien-1-ylidene) hydrazine (**3k**).* Brown solid (48% yield): Rf = 0.6 (hexane/ethyl acetate, 5:1, v/v); mp 147–149 °C; ^{1}H NMR (DMSO-d_6, 500 MHz) δ 11.64 (s, 1H), 7.59–7.56 (m, 2H), 7.30–7.26 (m, 2H); ^{13}C NMR ($CDCl_3$, 125 MHz) δ 160.0 (d, J_{CF} = 243.3 Hz, 1C), 137.8, 131.0, 130.9, 124.1, 119.4, 116.5 (d, J_{CF} = 23.1 Hz, 1C), 116.4 (d, J_{CF} = 7.9 Hz, 1C), 104.9; ^{19}F NMR ($CDCl_3$, 376 MHz, ^{1}H-dc) δ -117.44 ppm; DART-HRMS found 324.90593 $[M+H]^+$, calcd for $C_{11}H_6Cl_4FN_2$ 324.92691.

*2-(Perchlorocyclopenta-2,4-dien-1-ylidene)-1,1-diphenylhydrazine (**3l**).* Dark red solid (78% yield): Rf = 0.6 (hexane/ethyl acetate, 10:1, v/v); mp 128–130 °C; ^{1}H NMR (DMSO-d_6, 500 MHz) δ 7.48 (t, J = 7.5 Hz, 4H), 7.37 (t, J = 7.0 Hz, 2H), 7.34 (d, J = 7.5 Hz, 4H); ^{13}C NMR (DMSO-d_6, 125 MHz) δ 146.5, 132.2, 131.7, 130.4, 128.3, 123.6, 123.0, 121.7, 106.4 ppm; DART-HRMS found 381.95616 $[M]^+$, calcd for $C_{17}H_{10}Cl_4N_2$ 381.95981.

Representative procedure for synthesis of mono and diacyl hydrazones

*Method A. N′-(Perchlorocyclopenta-2,4-dien-1-yli-dene)benzohydrazide (**4a**).* To a solution of (perchloro-cyclopenta-2,4-dien-1-ylidene)hydrazine (**B**, 116 mg, 0.5 mmol, 1.0 eq) in tetrahydrofuran (10 mL) was added benzoic anhydride (113 mg, 0.5 mmol, 1.0 eq) and triethylamine (0.07 mL, 0.5 mmol, 1.0 eq) dropwise in ice-bath. The reaction mixture was stirred for 3 h at room temperature and then concentrated in vacuo. The residue was diluted with ethyl acetate (150 mL) and washed with water (2 × 50 mL) and brine (50 mL). The organic layer was dried with MgSO4, filtered and concentrated in vacuo. The residue was purified by flash column chromatography over silica gel (hexane/ethyl acetate, 10:1, v/v) to afford the desired product **4a** (239 mg, 71%) as brown solid: Rf = 0.45 (hexane/ethyl acetate, 5:1, v/v); mp 170–172 °C; ^{1}H NMR (DMSO-d_6, 500 MHz) δ 11.98 (s, 1H), 7.93 (d, J = 7.5 Hz, 2H), 7.69 (t, J = 7.5 Hz, 1H), 7.59 (t, J = 7.5 Hz, 2H); ^{13}C NMR (DMSO-d_6, 125 MHz) δ 164.8, 140.8, 135.0, 133.7, 132.1, 129.5, 129.3, 128.7, 120.8, 109.7 ppm; DART-HRMS found 334.91239 $[M+H]^+$, calcd for $C_{12}H_7Cl_4N_2O$ 334.93125.

*N-Benzoyl-N′-(perchlorocyclopenta-2,4-dien-1-ylidene)benzohydrazide (**4b**).* Dark brown solid (52% yield): Rf = 0.65 (hexane/ethyl acetate, 5:1, v/v); mp 123–124 °C; ^{1}H NMR ($CDCl_3$, 500 MHz) δ 7.15 (dd, J = 8.5, 1.0 Hz, 2H), 8.02 (dd, J = 8.5, 1.0 Hz, 2H), 7.68 (tt, J = 7.5, 1.0 Hz, 1H), 7.56 (t, J = 7.5 Hz, 1H), 7.53 (t, J = 7.5 Hz, 2H), 7.48 (t, J = 7.5 Hz, 2H); ^{13}C NMR ($CDCl_3$, 125 MHz) δ 162.1, 151.0, 149.4, 137.7, 134.4, 132.6, 132.5, 130.6, 130.0, 128.9, 128.8, 128.1, 127.6, 120.2, 112.4 ppm; DART-HRMS found 438.93702 $[M+H]^+$, calcd for $C_{19}H_{11}Cl_4N_2O_2$ 438.95747.

*N′-(Perchlorocyclopenta-2,4-dien-1-ylidene)aceto-hydrazide (**4c**).* Brown solid (89% yield): Rf = 0.7 (hexane/ethyl acetate, 5:1, v/v); mp 145–147 °C; ^{1}H NMR ($CDCl_3$, 500 MHz) δ 10.62 (s, 1H), 2.42 (s, 3H); ^{13}C NMR ($CDCl_3$, 125 MHz) δ 173.6, 136.3, 135.1, 129.1, 120.9, 107.5, 19.6 ppm; DART-HRMS found 272.89722 $[M+H]^+$, calcd for $C_7H_4Cl_4N_2O$ 272.91560.

*N′-(Perchlorocyclopenta-2,4-dien-1-ylidene)pivalohydrazide (**4d**).* Red brown solid (71% yield): Rf = 0.5 (hexane/ethyl acetate, 5:1, v/v); mp 156–158 °C; ^{1}H NMR (DMSO-d_6, 500 MHz) δ 11.17 (s, 1H), 1.24 (s, 9H); ^{13}C NMR (DMSO-d_6, 125 MHz) δ 175.4, 139.5, 134.5, 128.7, 120.7, 109.3, 39.3, 27.0 ppm; DART-HRMS found 314.94314 $[M+H]^+$, calcd for $C_{10}H_{11}Cl_4N_2O$ 314.96255.

*4-Fluoro-N-(4-fluorobenzoyl)-N′-(perchlorocyclo-penta-2,4-dien-1-ylidene)benzohydrazide (**4e**).* Brown solid (67% yield): Rf = 0.75 (hexane/ethyl acetate, 5:1, v/v); mp 126–128 °C; ^{1}H NMR ($CDCl_3$, 500 MHz) δ 8.17 (dd, J = 8.5, 5.0 Hz, 2H), 8.03 (dd, J = 9.0, 5.0 Hz, 2H), 7.20 (t, J = 9.0 Hz, 2H), 7.17 (t, J = 8.5 Hz, 2H); ^{13}C NMR ($CDCl_3$, 125 MHz) δ 166.6 (d, J_{CF} = 255.4 Hz, 1C), 165.5 (d, J_{CF} = 253.5 Hz, 1C), 161.1, 150.9, 149.9, 138.0, 133.4 (d, J_{CF} = 9.6 Hz, 1C), 132.8, 130.6 (d, J_{CF} = 9.0 Hz, 1C), 126.2 (d, J_{CF} = 3.0 Hz, 1C), 123.7 (d, J_{CF} = 2.9 Hz, 1C), 120.2, 116.3 (d, J_{CF} = 9.3 Hz, 1C), 116.2 (d, J_{CF} = 9.3 Hz, 1C), 112.3; ^{19}F NMR ($CDCl_3$, 376 MHz, ^{1}H-dc) δ -102.42, -105.37 ppm; DART-HRMS found 474.91973 $[M+H]^+$, calcd for $C_{19}H_9Cl_4F_2N_2O_2$ 474.93862.

*4-Methyl-N-(4-methylbenzoyl)-N′-(perchlorocyclo-penta-2,4-dien-1-ylidene)benzohydrazide (**4f**).* Brown solid (48% yield): Rf = 0.75 (hexane/ethyl acetate, 5:1, v/v); mp 147–149 °C; ^{1}H NMR ($CDCl_3$, 500 MHz) δ 8.03 (d, J = 8.0 Hz, 2H), 7.91 (d, J = 8.0 Hz, 2H), 7.31 (d, J = 8.0 Hz, 2H), 7.27 (d, J = 10.5 Hz, 2H), 2.46 (s, 3H), 2.42 (s, 3H); ^{13}C NMR ($CDCl_3$, 125 MHz) δ 162.2, 151.8, 149.4, 145.3, 143.3, 137.5, 132.3, 130.7, 129.7, 129.5, 128.2, 127.4, 127.9, 120.2, 112.3 ppm; DART-HRMS found 466.97013 $[M+H]^+$, calcd for $C_{21}H_{15}Cl_4N_2O_2$ 466.98877.

*Method B. tert-Butyl 2-(perchlorocyclopenta-2,4-dien-1-ylidene) hydrazine-1-carboxylate (**4g**).* To a solution of (perchlorocyclopenta-2,4-dien-1-ylidene)hydrazine (**B**, 116 mg, 0.5 mmol, 1.0 eq) in tetrahydrofuran (10 mL) was added pyridine (0.04 mL, 0.5 mmol, 1.0 eq) and 4-dimethylaminopyridine (12 mg, 0.1 mmol, 0.2 eq) at room temperature and the mixture was cooled down in ice bath. To the mixture, di-*tert*-butyl dicarbonate (164 mg, 0.75 mmol, 1.5 eq) in tetrahydrofuran (2 mL) was added dropwise at 0 °C. The ice bath was removed and the reaction mixture was allowed to warm to room temperature and stirred for 16 h at room temperature and then concentrated in vacuo. The residue was diluted with ethyl acetate (100 mL) and washed with water (2 × 30 mL) and brine (30 mL). The organic layer was dried with MgSO4, filtered and concentrated in vacuo. The residue was purified by flash column chromatography over silica gel (hexane/ethyl acetate, 20:1, v/v) to afford the desired product **4h** (90 mg, 54%) as orange solid: Rf = 0.5 (hexane/ethyl acetate, 5:1, v/v); mp 108–110 °C; ^{1}H NMR ($CDCl_3$, 500 MHz) δ 10.22 (s, 1H), 1.56 (s, 9H); ^{13}C NMR ($CDCl_3$, 125 MHz) δ 150.5, 135.9, 135.7, 128.2, 121.4, 107.2, 84.2, 28.0 ppm; DART-HRMS found 330.95319 $[M+H]^+$, calcd for $C_{10}H_{11}Cl_4N_2O_2$ 330.95747.

*Prop-2-yn-1-yl 2-(perchlorocyclopenta-2,4-dien-1-ylidene)hydrazine-1-carboxylate (**4h**).* Red solid (19% and 30% RSM): Rf = 0.5 (hexane/ethyl acetate, 5:1, v/v); mp 170–172 °C; ^{1}H NMR ($CDCl_3$, 500 MHz) δ 10.37 (s, 1H), 4.91 (d, J = 2.5 Hz, 2H), 2.58 (t, J = 2.5 Hz, 1H); ^{13}C NMR ($CDCl_3$, 125 MHz) δ 151.3, 137.4, 136.9, 129.2,

121.5, 107.4, 76.5, 76.3, 54.6 ppm; DART-HRMS found 312.90698 $[M+H]^+$, calcd for $C_9H_5Cl_4N_2O_2$ 312.91052.

*2-Methylbut-3-yn-2-yl 2-(perchlorocyclopenta-2,4-dien-1-ylidene)hydrazine-1-carboxylate (**4i**).* Red solid (50% yield): Rf = 0.5 (hexane/ethyl acetate, 5:1, v/v); mp 143–145 °C; ^1H NMR ($CDCl_3$, 500 MHz) δ 10.27 (s, 1H), 2.62 (s, 1H), 1.80 (s, 6H); ^{13}C NMR ($CDCl_3$, 125 MHz) δ 149.9, 136.6, 136.2, 128.6, 121.5, 107.3, 83.5, 75.2, 73.6, 28.9 ppm; DART-HRMS found 340.98938 $[M+H]^+$, calcd for $C_{11}H_9Cl_4N_2O_2$ 340.94182.

*(9H-Fluoren-9-ylidene)hydrazine (**6a**).* To an ethanol (10 mL) solution of fluoren-9-one (360 mg, 2.0 mmol, 1.0 eq) was added hydrazine monohydrate (0.29 mL, 6.0 mmol, 3.0 eq) dropwise at room temperature. The reaction mixture was refluxed for 6 h and then concentrated in vacuo. The residue was diluted with ethyl acetate (100 mL) and washed with water (2 × 30 mL) and brine (40 mL). The organic layer was dried with MgSO4, filtered and concentrated in vacuo. The residue was purified by flash column chromatography over silica gel (hexane/ethyl acetate, 10:1, v/v) to afford the desired product **6a** (315 mg, 81%) as yellow solid: Rf = 0.15 (hexane/ethyl acetate, 10:1, v/v); mp 152–154 °C; ^1H NMR ($CDCl_3$, 500 MHz) δ 7.91 (d, J = 7.5 Hz, 1H), 7.77 (d, J = 7.5 Hz, 1H), 7.73 (d, J = 7.0 Hz, 1H), 7.65 (d, J = 7.5 Hz, 1H), 7.44 (t, J = 7.5 Hz, 1H), 7.37–7.29 (d, 3H), 6.41 (s, 2H); ^{13}C NMR ($CDCl_3$, 125 MHz) δ 145.6, 141.3, 138.6, 137.7, 130.2, 129.7, 128.5, 127.9, 127.7, 125.5, 120.8, 120.5, 119.5 ppm; DART-HRMS found 195.09088 $[M+H]^+$, calcd for $C_{13}H_{11}N_2$ 195.09222.

*(9H-Xanthen-9-ylidene)hydrazine (**6b**).* Yellow solid (21% yield): Rf = 0.3 (hexane/ethyl acetate, 5:1, v/v); mp 126–128 °C; ^1H NMR ($CDCl_3$, 500 MHz) δ 8.32 (d, J = 8.0 Hz, 1H), 7.91 (d, J = 7.5 Hz, 1H), 7.43 (t, J = 7.5 Hz, 1H), 7.34–7.30 (m, 2H), 7.21 (t, J = 7.5 Hz, 1H), 7.18–7.15 (m, 2H), 5.80 (br, 2H); ^{13}C NMR ($CDCl_3$, 125 MHz) δ 154.0, 151.8, 135.9, 130.8, 129.4, 127.4, 124.1, 123.9, 123.3, 122.6, 118.2, 117.5, 116.5 ppm; DART-HRMS found 211.08521 $[M+H]^+$, calcd for $C_{13}H_{11}N_2O$ 211.08714.

*1-(9H-Fluoren-9-ylidene)-2-(3-fluorophenyl)hydrazine (**6d**).* To an ethanol (10 mL) suspension of 3-fluorophenylhydrazine HCl (325 mg, 2.0 mmol, 2.0 eq) was added triethylamine (0.29 mL. 2.1 mmol, 2.1 eq) and the mixture was stirred for 0.5 h. To the reaction mixture was added fluoren-9-one (180 mg, 1.0 mmol, 1.0 eq) and refluxed for 24 h. After the completion, the mixture was concentrated in vacuo. The residue was diluted with ethyl acetate (100 mL) and washed with water (2 × 30 mL) and brine (40 mL). The organic layer was dried with MgSO4, filtered and concentrated in vacuo. The residue was purified by flash column chromatography over silica gel (hexane/ethyl acetate, 10:1, v/v) to afford the desired product **6d** (242 mg, 84%) as brown solid: Rf = 0.4 (hexane/ethyl acetate, 5:1, v/v); mp 159–161 °C; ^1H NMR ($CDCl_3$, 500 MHz) δ 8.80 (s, 1H), 7.90–7.88 (m, 1H), 7.83 (d, J = 8.0 Hz, 1H), 7.78 (d, J = 7.5 Hz, 1H), 7.66–7.65 (m, 1H), 7.45 (td, J = 7.5, 0.5 Hz, 1H), 7.39–7.27 (m, 4H), 7.18 (dt, J = 11.0, 2.5, 1H), 6.98 (dd, J = 8.0, 2.0 Hz, 1H), 6.68 (td, J = 8.5, 2.5 Hz, 1H); ^{13}C NMR ($CDCl_3$, 125 MHz) δ 164.0 (d, J_{CF} = 242.8 Hz, 1C), 146.2 (d, J_{CF} = 10.6 Hz, 1C), 141.5, 141.0, 138.1, 137.7, 130.5 (d, J_{CF} = 9.8 Hz, 1C), 130.1, 129.8, 128.5, 128.0, 127.6, 124.4, 121.1, 120.9, 119.6, 109.3 (d, J_{CF} = 2.5 Hz, 1C), 108.2 (d, J_{CF} = 21.6 Hz, 1C), 101.0 (d, J_{CF} = 26.5 Hz, 1C) ppm; DART-HRMS found 289.11254 $[M+H]^+$, calcd for $C_{19}H_{14}FN_2$ 289.11355.

*tert-Butyl 2-(9H-fluoren-9-ylidene)hydrazine-1-carboxylate (**6e**).* To a solution of (9*H*-Fluoren-9-ylidene)hydrazine (**6a**, 97 mg, 0.5 mmol, 1.0 eq) in tetrahydrofuran (8 mL) was added pyridine (0.04 mL, 0.5 mmol, 1.0 eq) and DMAP (12 mg, 0.1 mmol, 0.2 eq) at room temperature, and the mixture was cooled with an ice-bath. To the mixture, di-*tert*-butyl dicarbonate (164 mg, 0.75 mmol, 1.5 eq) in tetrahydrofuran (2 mL) was added dropwise at 0 °C. The ice bath was removed and the reaction mixture was allowed to warm to room temperature and stirred for 3 h at room temperature and then concentrated in vacuo. The residue was diluted with ethyl acetate (100 mL) and washed with water (2 × 30 mL) and brine (30 mL). The organic layer was dried with MgSO4, filtered and concentrated in vacuo. The residue was purified by flash column chromatography over silica gel (hexane/ethyl acetate, 10:1, v/v) to afford the desired product **6e** (96 mg, 65%) as yellow solid: Rf = 0.5 (hexane/ethyl acetate, 5:1, v/v); mp 106–107 °C; ^1H NMR ($CDCl_3$, 500 MHz) δ 8.85 (s, 1H), 7.93 (d, J = 7.5 Hz, 1H), 7.79 (d, J = 8.0 Hz, 1H), 7.74 (d, J = 7.5 Hz, 1H), 7.61 (d, J = 7.5 Hz, 1H), 7.47 (t, J = 7.5 Hz, 1H), 7.38–7.35 (m, 2H), 7.31 (t, J = 7.5 Hz, 1H), 1.61 (s, 9H); ^{13}C NMR ($CDCl_3$, 125 MHz) δ 152.8, 146.1, 142.4, 139.1, 137.1, 130.9, 129.9, 129.8, 128.3, 127.9, 125.3, 122.3, 120.9, 119.5, 82.4, 28.3 ppm; DART-HRMS found 295.14353 $[M+H]^+$, calcd for $C_{18}H_{19}N_2O_2$ 295.14353.

*2,3,4,5-Tetrachlorocyclopenta-2,4-dien-1-one oxime (**7a**).* To hydroxylamine HCl (417 mg, 6.0 mmol, 6.0 eq) in 50 mL-round bottomed flask was added methanol (5 mL) and potassium hydroxide (337 mL, 6.0 mmol, 6.0 eq) in methanol (5 mL) at room temperature and the mixture was stirred for 1 h. Then the resultant KCl was filtered and the hydroxylamine solution was added to hexachlorocyclopentadiene (0.16 mL, 1.0 mmol, 1.0 eq) in methanol (5 mL) dropwise, and the mixture was refluxed for 6 h. After all hexachlorocyclopentadiene was consumed, the mixture was concentrated in vacuo. The residue was purified by flash column chromatography over silica gel (hexane/ethyl acetate, 10:1, v/v) to afford the desired product **7a** (80 mg, 34%) as red brown solid: Rf = 0.5 (hexane/ethyl acetate, 5:1, v/v); mp 178–180 °C; ^1H NMR (DMSO-d_6, 500 MHz) δ 14.52 (s, 1H); ^{13}C NMR (DMSO-d_6, 125 MHz) δ 145.8, 134.2, 128.3, 119.0, 109.3 ppm; DART-HRMS found 231.87045 $[M+H]^+$, calcd for C_5HCl_4NO 231.88905.

*1,2,3,4-Tetrachloro-5,5-dimethoxycyclopenta-1,3-diene (**7b**).* To a methanol (5 mL) solution of hexachlorocyclopentadiene (0.48 mL, 3.0 mmol, 1.0 eq) was added potassium hydroxide (370 mL, 6.6 mmol, 2.2 eq) in methanol (5 mL) dropwise for 30 min at room temperature. The mixture was stirred for 18 h and the mixture was poured to chopped ice (70 mL). After the ice had melted, the mixture was extracted with dichloromethane (3 × 100 mL). The organic layer was dried with brine (100 mL) and MgSO4, filtered and concentrated in vacuo. The residue was purified by flash column chromatography over silica gel (hexane/ethyl acetate, 10:1, v/v) to afford the desired product **7b** (230 mg, 29%) as light brown oil: Rf = 0.15 (hexane/ethyl acetate, 10:1, v/v); ^1H NMR ($CDCl_3$, 500 MHz) δ 3.34 (s, 6H); ^{13}C NMR ($CDCl_3$, 125 MHz) δ 129.4, 128.5, 104.8, 51.9 ppm.

Biological methods

Cell lines

The 8226 and MM1.S myeloma cell lines were purchased from ATCC. The cell lines were characterized by FISH analysis and shown to contain MAF/Ig translocations. Western blot confirmed a significant over-expression of DEPTOR protein. Both lines were tested for mycoplasma within the last 6 months and were negative.

Western blot assay

Protein was extracted and separated by 12.5% SDS-PAGE as previously described.[14] Proteins were transferred to polyvinylidene difluoride membranes and their expression was detected utilizing specific antibodies purchased from Cell Signaling (Beverly, MA).

MTT assay

The MTT assay was performed by seeding 1–2 × 10^4 target cells in 0.1 ml of complete media into wells of a 96 well microtiter plate. After incubation with compounds, the reduction of MTT to formazan by live cells was determined with a microplate ELISA reader equipped with a 570 nm filter. Quadrupliate wells were run for each group and the SD of each group was always <5% of the mean. Results are presented as% of control or% survival where OD of exp group was compared to the OD of a control group (cells incubated with DMSO alone) where the latter was arbitrarily made to be 100%.

Apoptosis assay

To identify apoptotic cells, we used a phycoerythrin (PE)-conjugated antibody specific for activated caspase 3 (BD Biosciences). For staining, 10^6 cells were washed with PBS and fixed and permeabilized with 0.5 ml cytofix/cytoperm solution. The cells were then incubated with a 1:5 dilution of PE-conjugated monoclonal anti-caspase 3 antibody for 30 min and analyzed by flow cytometry.

RAPTOR knockdown

The short hairpin RNAs (shRNA)/pLKO.1, targeting RAPTOR or a scrambled sequence (control) were obtained from Addgene. Lentivirus was produced by the UCLA Vector Core facility and stable cell lines were made by transducing cells with lentivirus and selecting in geneticin.

Statistical analysis

The induction of p70 phosphorylation by derivative compounds was determined by densitometry, comparing immunoblot signals of phosphorylated p70 vs total p70. This ratio was then compared to that resulting from parental compound B, with the latter ratio arbitrarily placed at '1'. The IC_{50} for MTT cytotoxicity was determined using a range of concentrations of derivatives. Percent apoptosis was enumerated by flow cytometry in drug-treated cultures by subtracting control apoptosis determined from DMSO-treated cultures. The percent apoptosis (i. e., positive staining for activated caspase 3) in the DMSO control cultures was always <15%.

Author contributions

All authors contributed to the writing of this manuscript. All authors have given approval to the final version of the manuscript.

Notes

The authors declare no competing financial interest. M.E.J., J.L., A.L., Y.S. and J.G. are coauthors on a patent application that includes the molecules described in this manuscript.

Acknowledgments

This study was supported by NIH grants 2RO1CA111448, RO1CA168700, R21CA168491, RO1CA211562 as well as research funds of the Veteran's Administration and the Multiple Myeloma Research Foundation. The NMR spectrometers were supported by the National Science Foundation under equipment grant no. CHE-1048804.

A. Supplementary data

Supplementary data associated with this article can be found, in the online version, at http://dx.doi.org/10.1016/j.bmcl.2017.09.002.

References

1. Peterson TR, Laplante M, Thoreen CC, et al. DEPTOR is an mTOR inhibitor frequently overexpressed in multiple myeloma cells and required for their survival. *Cell*. 2009;137:873–886.
2. Carrasco DR, Tonon G, Huang Y, Zhang Y, Sinha R, Feng B. High resolution genomic profiles define distinct clinico-pathogenetic subgroups of multiple myeloma patients. *Cancer Cell*. 2006;9:313–325.
3. Yang Y, Bardeleben C, Frost P, et al. DEPTOR is linked to a TORC1-p21 survival proliferation pathway in multiple myeloma cells. *Genes Cancer*. 2014;5:407–419.
4. Shi Y, Daniels-Wells T, Frost P, et al. Cytotoxic properties of a DEPTOR-mTPR inhibitor in multiple myeloma cells. *Cancer Res*. 2016;76:5822–5831.
5. Hafner K, Schulz G, Wagner K. Cyclisch konjugierte 5- und 7-Ringsysteme I. 6-Amino- sowie 6-Hydroxy-fulvene und deren Aza-analoga. *Liebigs Ann Chem*. 1964;678:39–53.
6. Disselnkotter H. Tetrachlor-diazo-cyclopentadien aus Hexachlor-cyclopentadien. *Angew Chem*. 1964;76:431–432.
7. For a discussion of the source of the color of these compounds and other analogues, see: Griffiths J, Lockwood M. Chromogens based on non-benzenoid aromatic systems. Part III. synthesis, spectra, and molecular orbital calculations in the substituted fulvene and 6-azafulvene series. *J Chem Soc, Perkin Trans 1*. 1976;48–54.
8. Dixon DD, Ford ME. Preparation of N-Acyl substituted tetrachlorocyclopentadienone hydrazones. *Synthesis*. 1980;306–308.
9. Bartucci MA, Wierzbicki PM, Gwengo C, Shajan S, Hussain SH, Ciszek JW. Synthesis of dihydroindolizines for potential photoinduced work function alteration. *Tetrahedron Lett*. 2010;51:6839–6842.
10. Hafiz M, Taylor GA. Keten. Part 17. Addition reactions of ketens with N-phenyl nitrones. *J Chem Soc, Perkin Trans 1*. 1980;1700–1705.
11. Garcia-Ramos Y, Proulx C, Lubell WD. Synthesis of hydrazine and azapeptide derivatives by alkylation of carbazates and semicarbazones. *Can J Chem*. 2012;90:985–993.
12. A discussion of this novel finding will be the subject of an upcoming manuscript.
13. Malihi F, Clive DLJ, Chang CC. Minaruzzaman. Synthetic studies on CP-224,917 and CP-263,114: Access to advanced tetracyclic systems by intra-molecular conjugate displacement and [2,3]-Wittig rearrangement. *J Org Chem*. 2013;78:996–1013.
14. Tu Y, Gardner A, Lichtenstein A. The phosphatidylinositol 3-kinase/AKT kinase pathway in multiple myeloma plasma cells: Roles in cytokine-dependent survival and proliferative responses. *Cancer Res*. 2000;60:6763–6770.